Earth and Planetary Science Letters 284 (2009) 144–150

Contents lists available at ScienceDirect

Earth and Planetary Science Letters

journal homepage: www.elsevier.com/locate/epsl

A multi-phase model of runaway core–mantle segregation in planetary embryos

Yanick Ricard [a,*], Ondřej Šrámek [b], Fabien Dubuffet [a]

[a] Laboratoire des Sciences de la Terre, Université de Lyon, CNRS UMR5570, Batiment Géode, 2 rue Raphael Dubois, 69622, Villeurbanne Cedex, France
[b] Department of Geophysics, Faculty of Mathematics and Physics, Charles University in Prague, V Holešovičkách 2, 180 00 Praha, Czech Republic

ARTICLE INFO

Article history:
Received 26 November 2008
Received in revised form 1 April 2009
Accepted 15 April 2009
Available online 22 May 2009
Editor: T. Spohn

Keywords:
core formation
multiphase flow
planetary formation

ABSTRACT

A classic scenario of core formation suggests that growing proto-planets are heated by the impacts of accreting planetesimals at their surface until their shallow layers reach the melting temperature of their metallic components or even of the silicates. In this partially molten shell, metal and silicates differentiate and the metallic phase ponds on top of the still undifferentiated inner planet. Later a gravitational instability brings dense metallic diapirs to the center of the planet. We test this multi-phase scenario by using a formalism that self-consistently accounts for the presence of solid silicates, solid and liquid iron. At each point of the mixture an average velocity and a separation velocity of the solid and liquid phases are defined. The energy balance accounts from the changes in potential energy associated with the segregation. We show that core formation starts before a significant melting of the silicates, as soon as impact heating is large enough to reach the melting temperature of the metallic component. Segregation proceeds in a few thousand years by a runaway process due to the conversion of gravitational energy into heat that occurs necessarily in all undifferentiated embryos of Moon to Mars sizes. The first metallic diapirs leave behind them a trailing conduit along which most of the further melting occurs. The cores of large planets do not form at the end of accretion but must result from the merging of the already differentiated hot cores of embryos.

1. Introduction

After condensation of the first solids in a nebula, the rocky grains coagulate near the central star to form small planetesimals (Kokubo and Ida, 1996). After a few 100 kyrs, the distribution of planetesimals is dominated by a few tens of moon-sized oligarchs (Kokubo and Ida, 1998). The terrestrial planets are then built by the violent merging of these oligarchs (Canup and Asphaug, 2001) resulting from their gravitational interactions. One of the late collision led to the formation of the Moon (around 60 Myr, Touboul et al., 2007). The segregation of Earth's core constrained by Hf–W timings has taken place with a mean age around 30 Myr (Yin et al., 2002) before the end of the accretion (around 100 Myr).

Small planetesimals have undergone early melting events due to the presence of short period radioactivities (Carlson and Langmuir, 2000). However, a widely accepted model initiates large scale core–mantle differentiation in planetary embryos from a shallow magma ocean generated by the heat deposited by the impacts of the accreting planetesimals (Kaula, 1979; Benz and Cameron, 1990; Tonks and Melosh, 1993; Rubie et al., 2003). In this partially molten shell, metal and silicates differentiate and the metallic phase ponds on top of the still undifferentiated inner planet. Later a gravitational instability brings dense metallic diapirs to the center of the planet (Stevenson, 1990). This scenario is supported by moderately siderophile element systematics (Li and Agee, 1996) and by simple physical arguments (Solomatov, 2000). However, up to now, it lacks a self consistent physical framework that requires simultaneously handling two components, metal and silicates, and two phases, solid and liquid (in this paper we reserve the word "phase" for the physical state, solid or liquid, and the word "component" for the chemical composition, metal or silicate). Previous attempts to simulate numerically the segregation, have made large simplifications, given the multi-phase non-Boussinesq mixture (i.e. where the density variations are comparable to the density itself) by considering it as a single Boussinesq fluid (e.g., Honda et al., 1993; Höink et al., 2006), or by considering that the whole metal component is liquid (e.g., Golabek et al., 2008). A number of issues remain therefore unclear, in particular, the dynamics of this segregation, continuous or punctuated, and whether the formation started in planetary embryos at the beginning of the oligarchic growth period or at the late stages of accretion. In this paper, we propose an attempt to answer these problems by using for the first time, a general multi-phase formalism that we developed in a series of papers (Bercovici et al., 2001; Bercovici and Ricard, 2003; Šrámek et al., 2007).

2. Impact energy and core segregation energy

It has been known for a long time that two energies are relevant to the post-impact dynamics. One is the energy buried by the impactor inside the planet (Tonks and Melosh, 1993), the other is the gravitational energy release by the core segregation (Flasar and Birch, 1973; Solomon, 1979).

When an impactor of mass m_i strikes a planet, a fraction f_1 of its kinetic energy is buried into a domain of mass $m = f_2 m_i$. The rest of the kinetic energy is rapidly radiated away and may heat up the primitive

* Corresponding author.
E-mail address: ricard@ens-lyon.fr (Y. Ricard).

0012-821X/$ – see front matter © 2009 Elsevier B.V. All rights reserved.
doi:10.1016/j.epsl.2009.04.021

atmosphere (Matsui and Abe, 1986a). The two factors f_1 and f_2 are not well known but have been estimated from experiments and models to be $f_1 \sim 1/3$ and $f_2 \sim 6$, i.e., one third of the kinetic energy heats up rather homogeneously a volume 6 times larger than that of the impactor (Pierazzo et al., 1997; Monteux et al., 2007). The volume heated by the impact shock wave is roughly spherical and is tangent to the surface just below the impact point (Melosh, 1996). The escape velocity of a growing planet of radius R and surface gravity g, $\sqrt{2gR}$, should be indicative of the average impact velocity. We consider that the growing planet is undifferentiated with an average density $\bar{\rho} = \phi\,\rho_f + (1-\phi)\,\rho_m$ (ρ_f and ρ_m are the densities of metal and silicates, ϕ the volume proportion of metal). As $g = 4/3\pi G\bar{\rho}R$, where G is the gravitational constant and the average density, the energy density transferred to the impacted planet (energy per unit mass of the heated zone) is therefore

$$\Delta e_1 = \frac{4\pi f_1}{3 f_2}\bar{\rho} G R^2. \tag{1}$$

This amounts to Δe_1 [J kg^{-1}] $\sim 6.4\ 10^{-2}\ R^2$ [km^2]. For example, assuming the iron does not melt, this corresponds to a temperature increase of 260 K for a planet of 2000 km (all numerical values are listed in Table 1.). Alternatively, as soon as the planet reaches 1260 km, this energy δe_1 is enough to provide the latent heat $\rho_f \phi L / \bar{\rho}$ necessary to melt all the iron content of the impacted zone (L is the latent heat of iron melting and $\phi\,\rho_f/\bar{\rho}$ the mass proportion of metal).

The segregation of a undifferentiated planet with metal volume proportion ϕ and density $\bar{\rho} = \phi\,\rho_f + (1-\phi)\,\rho_m$ into a core of density ρ_f and a mantle of density ρ_m, is associated with a large change of gravitational energy (the gravitational energy is the generalization of the potential energy when the gravity field is time-dependent) and therefore releases the energy density (energy per unit mass of planet) (Flasar and Birch, 1973; Solomon, 1979)

$$\Delta e_2 = \frac{4G\pi R^2}{5\bar{\rho}}\left(\bar{\rho}^2 - \rho_f^2\phi^{5/3} - \rho_m^2\left(1-\phi^{5/3}\right) - \frac{5}{2}\left(\rho_f - \rho_m\right)\rho_m\phi\left(1-\phi^{2/3}\right)\right), \tag{2}$$

which cancels out for the three cases when segregation is not meaningful, $\phi = 0$ (no metal), $\phi = 1$ (no silicates) and $\rho_m = \rho_f$ (homogeneity). Typically for a planet containing 25% of metal in volume, Δe_2 [K] $\sim 5.8\ 10^{-2}\ R^2$ [km^2] (see parameters in Table 1.). Before iron melts, this increases the temperature by $\Delta T_2 \sim 240$ K for a planetary radius of $R = 2000$ km.

Table 1
Typical parameter values for numerical models of two phase segregation.

Planet radius	R	2000 km
Silicate density	ρ_m	3200 kg m^{-3}
Iron density	ρ_f	7000 kg m^{-3}
Heat capacity	C	1 kJ K^{-1} kg^{-1}
Heat conductivity	k_T	3 W m^{-1} K^{-1}
Initial temperature	T_0	1100 K
Iron melting temp.	$T_{\rm melt}$	1300 K
Initial metal content	ϕ_0	0.25
Silicate viscosity	μ_m	10^{19} Pa s
Solid iron viscosity	μ_m	10^{19} Pa s
Liquid iron viscosity	μ_f	1 Pa s
Permeability coeff.	k_0 ($k = k_0\phi^2$)	$4\ 10^{-9}$ m^2
Average density $\bar{\rho}$	$\phi\,\rho_f + (1-\phi_m)\,\rho_m$	4150 kg m^{-3}
Gravity	$g = 4\pi G\bar{\rho}R/3$	2.32 m s^{-2}
Temperature excess	ΔT	258 K
Temperature scale	$\theta = \Delta\rho g R/\rho C$	4247 K
Stokes velocity scale	$\Delta\rho g R^2/\mu_m$	111 km/yr
Time scale	$\mu_m/\Delta\rho g R$	18 yr
Darcy velocity	$k_0\Delta\rho g\phi_0^2(1-\phi_0)/\mu_f$	58 m/yr
Compaction length	$\delta\sqrt{k_0\mu_m/\mu_f}$	210 km
Norm. comp. length		0.1
Rayleigh number Ra	$\bar{\rho}\Delta\rho g C_p R^3/\eta_m k_T$	10^{10}

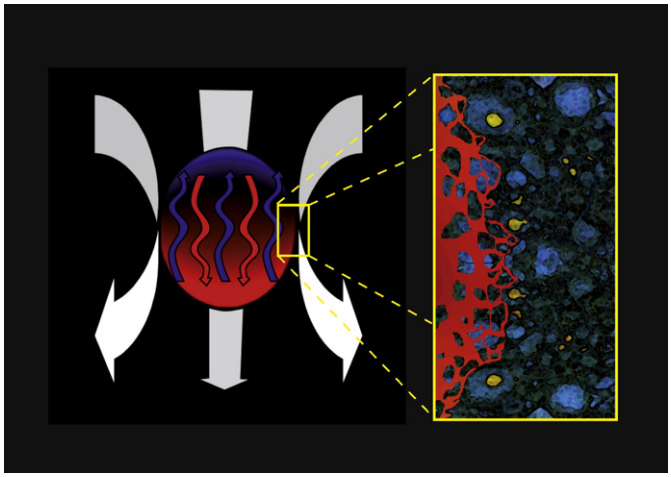

Fig. 1. Principle of the multi-phase formalism: at microscopic scale (shown in the insert), the undifferentiated planet is either cold and made of solid silicates and solid metal (right side), or above the metal melting temperature, $T_{\rm melt}$, and made of solid silicates (blue) and liquid metal (red). This microscopic physics when averaged over continuous variables leads to a macroscopic flow, superposition of a usual Stokes flow (white arrows) and a relative flow that segregates the dense metal (red) from the light residual silicates (blue), within the molten area. (For interpretation of the references to colour in this figure legend, the reader is referred to the web version of this article.)

The R^2 dependences and the comparability of the impact and core segregation energy densities have two consequences. Firstly, melting upon impact is rapidly inescapable as the energy density Δe_1 brought by impacts increases rapidly with R. Secondly, the differentiation of a given planetary volume initiated by an input of energy Δe_1 is potentially able to release enough gravitational energy, Δe_2, to melt the metal component of an equivalent undifferentiated volume. The first impact that induces metal melting can therefore initiate a runaway differentiation of a planet.

3. Multiphase equations for a metal-silicate continuum

A classical averaging approach combined with symmetry arguments is used to derive the mass, momentum, and energy equations of a mixture made of three different interacting materials: solid silicates, solid metal and liquid metal (McKenzie, 1984; Bercovici et al., 2001; Ricard et al., 2001; Bercovici and Ricard, 2003; Šrámek et al., 2007) (see Fig. 1). The three individual materials are considered as viscous, but the viscosities of the so called solid materials (the silicate and metal components in the solid phase) are infinitely larger (and equal for simplicity) than that of the liquid metal. At each point of the multiphase continuum the metal component is either totally in the solid state or totally liquid, but the metal can be solid in some parts of the planet and liquid in other parts. The simultaneous presence of two very different viscosities is a major numerical difficulty. We have not considered more complex rheologies like viscoelasticity or viscoplasticity.

The two components, metal and silicate, in volume proportions ϕ and $1-\phi$ have properties denoted by the subscripts f and m. These subscripts are in agreement with the previous derivation of two phase equations (Bercovici and Ricard, 2003; Šrámek et al., 2007) although in the present paper, the metallic phase (subscript f) is not necessarily fluid. The metal density, solid or liquid, is ρ_f and we call $\Delta\rho$ and Δv the differences of density and of volume averaged velocities between the silicate and metal components, $\rho_m - \rho_f$ and $v_m - v_f$. At each point in space, we define both a silicate velocity v_m and a metal velocity v_f that can be equal (when the metal is solid and locked in the silicates) or different (when the fluid metal can separate from the silicates). We non-dimensionalize lengths by the planet radius R, velocities by the two-phase Stokes velocity $|\Delta\rho|\ gR^2/\mu_m$, time by $\tau = \mu_m/(|\Delta\rho|gR)$, pressures by $|\Delta\rho|gR$ and temperatures by $\theta = |\Delta\rho|gR/(\bar{\rho}\bar{C})$.

The density difference between metal and silicates drives the flow and the velocity of each component v_m or v_f can be described macroscopically as the superposition of an incompressible and an irrotational velocity field (Spiegelman, 1993). The average momentum equation is

$$-\nabla\Pi + \nabla.\left[\mu^* \underline{\tau}\right] + \phi \boldsymbol{e}_g = 0, \tag{3}$$

where $\boldsymbol{e}_g$ is the vertical unit vector along gravity, $\underline{\tau}$ the viscous stresses, and Π is the average dynamic pressure. The flow is forced by the variations in metal content ϕ. The minor thermal buoyancy is neglected as much smaller than the compositional iron/silicate buoyancy. The stress tensor is simply related to the velocity of the solid component by

$$\underline{\tau} = \nabla v_m + \nabla^T v_m - \frac{2}{3}\nabla.v_m \underline{I} \tag{4}$$

The silicates are incompressible but the divergence of the volume average velocity $\nabla.v_m$, is not zero (McKenzie, 1984). The viscous stresses are only supported by the solid phase which implies that $\mu^*=1$ when the metal and silicates are solid, $\mu^*=1-\phi$ when the metal is liquid. The mixture viscosity therefore decreases linearly with the volume proportion of melt. The solid matrix viscosity is a very uncertain parameter. In earlier models, the deepest part of a growing planet was supposed to be rather cold and highly viscous (e.g. Honda et al., 1993; Senshu et al., 2002). However, these models neglected the presence of short period radionuclides like ^{26}Al of ^{60}Fe that heated very significantly the planet embryo and led to the melting of planetesimals a few million years after the beginning of condensation (Rubie et al., 2007). Furthermore, as the deviatoric stresses were large during differentiation, the real viscosity was likely nonlinear (Samuel and Tackley, submitted for publication). This leads us to use a rather low viscosity for the mixture, from 10^{19} Pa s in the absence of liquid metal, to potentially zero if only liquid metal is present.

In the regions where the metal is liquid it can separate from the silicates by percolation. Percolation of a fluid phase within a solid matrix occurs when the network of fluid pockets is connected. At low pressure, the metal does not "wet" the silicates and with a too low metal content, the liquid pockets should not connect (von Bargen and Waff, 1986). However, as soon as the metal content reaches ~3%, which is much lower than the average metal content of telluric planets, connection does occur (Yoshino et al., 2003). Deformation and pressure also favors the connection of the melt. We therefore assume that the liquid metal is connected, and for simplicity, even at vanishing porosity.

The fluid metal obeys a Darcy-type velocity

$$\Delta v = \delta^2 \phi \left(\nabla \left[\Pi + \frac{1-\phi}{\phi} \nabla.(\phi \Delta v) \right] - \boldsymbol{e}_g \right), \tag{5}$$

where δ is a compaction length. This equation assumes a permeability k of the silicate matrix varying as $k_0\phi^2$, where k_0 is a constant (see Bercovici et al., 2001). The dimensionless compaction length $\delta = \sqrt{k_0 \mu_m / \mu_f} / R$ is another uncertain parameter that we estimate as 0.1 in Table 1. A more general exploration of the parameter space k_0, μ_m, μ_f will have to be done in the future.

The term in $1/\phi$ represents the resistance to compaction (Bercovici and Ricard, 2003) equivalent to a bulk viscosity (McKenzie, 1984; Spiegelman, 1993). In other words, $\Pi + (1-\phi)\ \nabla.(\phi\Delta v)/\phi$ represents the fluid pressure acting on the fluid phase and driving the Darcy flow, sum of the average pressure Π and of a compaction term in $1/\phi$. When the temperature is below the iron melting temperature, $\delta=0$, and the two phases are locked together. Notice that the sinking of metallic droplets in low viscosity silicates (Höink et al., 2006) with a separation velocity Δv proportional to the density difference $\Delta\rho$ would correspond to a simpler version of Eq. (5) (it would suppress the resistance to compaction provided by the $1/\phi$ term).

These two momentum equations are supplemented by two mass conservation equations that can be written on the form

$$\nabla.v_m = \nabla.(\phi \Delta v), \tag{6}$$

and

$$\frac{D\phi}{Dt} = \nabla.[\phi(1-\phi)\Delta v], \tag{7}$$

where the Lagrangian derivative is with respect to the volume average mixture velocity, $\phi\ v_f + (1-\phi)\ v_m$. When the metal is solid, the two phases do not separate, the common velocity of the two solid components becomes incompressible and they are simply transported by the average flow.

The conversion of potential energy into heat is the fundamental ingredient accounted for by the energy equation. The energy equation writes

$$\frac{DT}{Dt} - \frac{1}{Ra}\nabla^2 T = \mu^* \tau : \nabla v_m + \frac{(\Delta v)^2}{\delta^2} + \frac{1-\phi}{\phi}(\nabla.v_m)^2. \tag{8}$$

The three sources of dissipation on the right side convert the changes of potential energy into heat: the dissipation by viscous shear, a Darcy friction related to the velocity difference between the silicates and liquid metal, and a compaction term coming from the resistance of the silicate matrix to isotropic deformation. The last two terms vanish when the metal is solid as Δv (see Eq. (5) with $\delta=0$) and thus $\nabla.v_m$ (see Eq. (6)) are both zero in this case.

Latent heat is neglected as a simplifying assumption, but is likely to have a small effect on the results. In particular, a comparison of the total latent heat stored in the molten metal to the total sensible heat stored in the two-phase mixture (i.e., $\rho_f \phi L / \bar{\rho}$ versus $\bar{\rho} C \delta T$) indicates an overestimation of temperature by $\delta T \sim 100$ K. As the melting temperature of iron containing impurities is ~60% lower than that of pure iron, this latent heat is probably overestimated by the same amount. Neglecting latent heat, the metal is locally either totally melted ($T > T_{melt}$) or totally solid ($T < T_{melt}$) depending on the temperature.

The set of multiphase equations is solved in 2D Cartesian geometry The velocities in the five 2D mechanical Eqs. (3), (5) and (6) are first replaced by a representation in terms of stream function and velocity potential, then solved by a finite volume method on a staggered grid (the numerical details and approximations are discussed in Sramek, 2007). The two transport Eqs. (7) and (8) are solved with an implicit, high accuracy, shock preserving scheme (Harten, 1983; Sramek, 2007).

A 2D Cartesian geometry is not appropriate for a self-coherent computation of the time dependent gravity field and our mechanical Eqs. (3) and (5) have assumed a uniform and constant gravity. This is an important simplification that misses the possible formation of the core by a so-called degree 1 instability (Stevenson, 1981; Honda et al., 1993; Gerya and Yuen, 2007), where while the metal is sinking, the undifferentiated material is simultaneously attracted up and around the dense metal. A complete 3D spherical model, where gravity will be computed from Poisson's equation will be needed but is yet far beyond the reach of our numerical code.

4. A model of core mantle segregation

We consider an impacted planet with an initial uniform gravity and composition (25% of iron). Its temperature resulting from the heating by short lived radionuclides at the planetesimal stage (Carlson and Langmuir, 2000) or from previous impacts, is $T_0 = 1100\ \mathrm{K} < T_{melt}$ except in a shallow circular zone where an impact raises the temperature

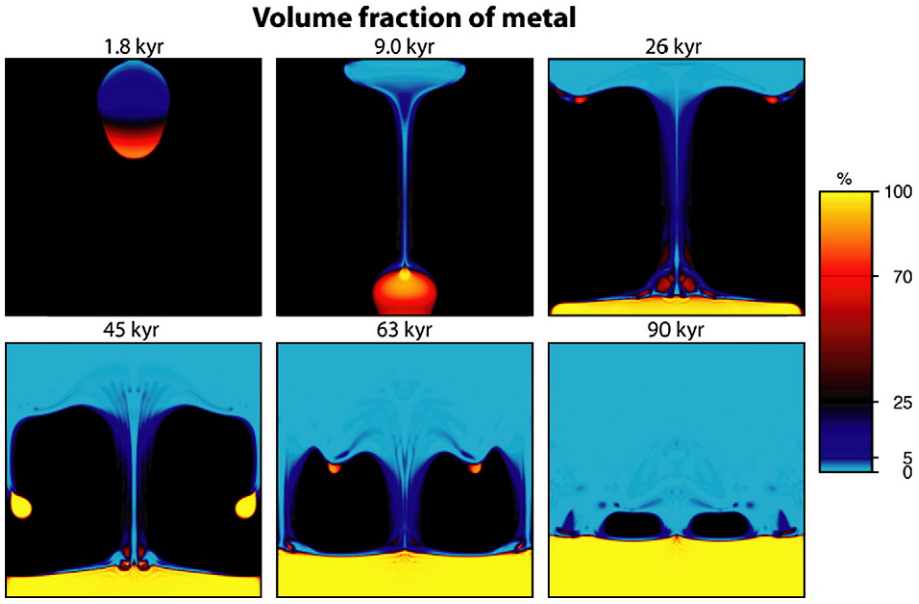

Fig. 2. Volume fraction of metal during core–mantle segregation: the undifferentiated planet is black, the differentiated silicates are blue, the metallic core, yellow. The initial planet is undifferentiated (black) and its temperature T_0 is below the iron melting temperature $T_{\rm melt}$ until the shock wave due to a meteoritic impact increases the temperature above $T_{\rm melt}$ in a shallow circular area. The metal segregates from silicates by a combined process of porous flow and diapiric instabilities. When the process is initiated, the release of gravitational energy provides enough heat to melt the whole metal component in ~110 kyr and to produce a solid silicated mantle (blue) and a liquid core (yellow). (For interpretation of the references to colour in this figure legend, the reader is referred to the web version of this article.)

above $T_{\rm melt}$. The radius of the heated zone is roughly two times that of the impactor (Tonks and Melosh, 1993). The evolution of the planet is then entirely controlled by the resolution of seven coupled differential equations, two vectorial, Eqs. (3) and (5), and three scalar, Eqs. (6), (7) and (8). The various parameters of the simulations are given in Table 1. This evolution is so rapid that we neglect the thermal diffusion at the surface which should, at any rate, be blanketed, at least partially, by a hot atmosphere (Matsui and Abe, 1986b).

Fig. 2 depicts several stages of segregation mechanisms from the impact ($t=0$) to the end of core formation ($t\sim110$ kyr) (see also a complete movie of this simulation in the supplementary material). Initially, the circular zone containing the molten metallic phase, segregates by a roughly 1-D porous compaction ($t\lesssim2$ kyr). The metal concentration increases in a dense blob that sinks eventually as a diapir (2–10 kyr). The gravitational energy released by the differentiation is converted into heat. The light residual silicate and the dense metal spread along the top and bottom surfaces, respectively (~26 kyr). A cusp-like channel connects the differentiated silicates to the core. This formation of trailing conduits has been documented experimentally (Olson and Weeraratne, 2008). New pockets of metal are formed and descend to the proto-core. At the interface between the differentiated silicates and the remaining undifferentiated mantle, new metallic ponds are formed (~26 kyr) that trigger secondary (30–50 kyr) and later tertiary (60–80 kyr) instabilities. After ~60 kyr, when only the deep mantle remains undifferentiated, the rate of release of potential energy decreases and the erosion of the last cold undifferentiated regions occurs by thermal diffusion. During the whole process, various compaction waves are visible in both the silicates and the core (Scott and Stevenson, 1984; Hier-Majumder et al., 2006).

The temperature evolution during segregation is depicted in Fig. 3. The dissipative heating occurs mostly along the channels trailing behind the diapirs. The maximum temperature reached in the simulation amounts to ~2000 K and occurs at 40 kyr. This increase of ~1000 K can be compared to two simple estimates. Each volume V of sinking metal releases the potential energy $\Delta\rho VgR$. An upper bound for the heating, ΔT_1, can be obtained by assuming that this energy is entirely transferred to the diapir on the form of the thermal energy $\rho_f VC\Delta T_1$. This leads to $\Delta T_1=(\Delta\rho gR)/(\rho_f C)=2520$ K. Our simulation suggests therefore that about 40% of the potential energy release is dissipated within the metallic diapirs and 60% in the surrounding material. A lower bound, ΔT_2 is obtained by releasing the potential energy, on average into the whole planet (this is equivalent, but for the Cartesian case, of the segregation energy given by Eq. (2)). On gets $\Delta T_2=(\Delta\rho gR)/(2\tilde{\rho}C)\phi(1-\phi)=398$ K. During segregation the local temperature increase can therefore reach about 2.5 times of the final average temperature increase.

With the low pressures involved in this planetary embryo, the maximum temperatures are enough to partially melt the silicates (the latent heat of silicate fusion would buffer this temperature). The extent of silicate melting remains however limited and most of the segregation occurs while the silicates are solid. Ultimately, similar high temperatures are reached in the core and in the shallow mantle. As we have neglected thermal expansion, no thermal convective instability occurs. This is reasonable for the silicates and the undifferentiated planet as the thermal density anomalies are very small and the segregation very fast. Thermal convection should occur in the liquid core and homogenize its temperature.

The fundamental ingredient of the runaway core formation predicted by our model is the comparable magnitude and R^2 dependence of the energies e_1 (1), brought by meteoritic impacts and e_2, (2), by release of gravitational energy. Although the extrapolation of 2-D modeling to 3-D spherical planets is difficult, we observe that even small impacts suffice to trigger the core-forming instability. We summarize different experiments in Fig. 4 as a function of the normalized radius of the impacted zone and the radius of the planetary embryo. The initial temperature T_0 in this experiment is 200 K below the iron melting temperature which is reached by impact heating when the planet has a radius of 1762 km (blue). For a large enough impacted zone (red), runaway core formation occurs. If impactors are too small, the iron melted by the impact re-solidifies (pink). As both the embryo and the impactor radii increase with time during the period of oligarchic growth, the system evolves always in the direction of the runaway melting instability.

This behavior can be understood by a simple physical interpretation. The initial diapir has a radius $R_{\rm D}$ and an excess temperature ΔT.

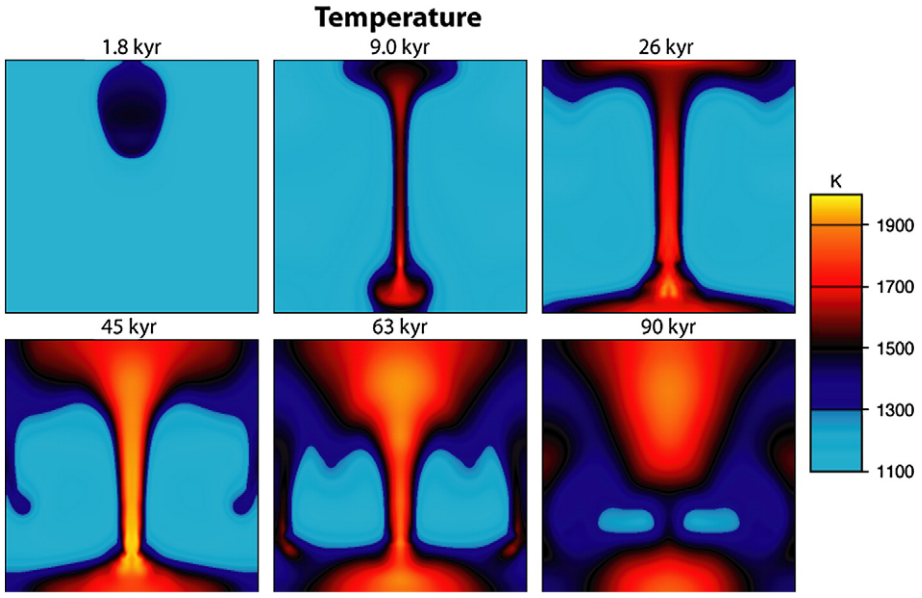

Fig. 3. Temperature during core–mantle segregation: the initial temperature T_0 is close to 1100 K and raised to 1400 K in the shallow impacted zone. The solid mixture (light blue) is below the metal melting temperature T_m of 1300 K. The further release of energy along the instability channels increases the temperature up to 2000 K (at ~40 kyr). At the end of the segregation, the shallow hot mantle should cool by convection while a hot proto-core remains thermally insulated by a cold lower mantle. (For interpretation of the references to colour in this figure legend, the reader is referred to the web version of this article.)

By thermal diffusion only, its maximum temperature decreases with time like $T(t) = T_0 + \Delta T\, erf\left(R_D / \left(2\sqrt{\kappa t}\right)\right)$ where κ is the thermal diffusivity. The diapir remains liquid until the time t_{diff} where $T(t_{diff}) = T_M$. This defines t_{diff} of order

$$t_{diff} \sim \frac{R_D^2}{4\kappa}\frac{\Delta T^2}{(T_M - T_0)^2}, \tag{9}$$

(the error function is quasi linear for $\Delta T > T_M - T_0$). Like the usual reasoning to get the Rayleigh criterion in simple Benard convection, the instability occurs if this diffusion time t_{diff} is long compared to the advection time scale $t_{adv} = R_D/v$, where v is the diapir sinking velocity (i.e., if the diapir has enough time to travel and to release gravitational energy before being thermally equilibrated). Using a Stokes law to estimate v,

$$t_{adv} \sim \frac{\mu_m}{\Delta\rho g R_D}. \tag{10}$$

The condition $t_{adv} \ll t_{diff}$ corresponds to

$$\frac{\Delta\rho g R_D^3}{4\mu_m\kappa}\frac{\Delta T^2}{(T_M - T_0)^2} = R_c >> 1, \tag{11}$$

which expresses that a dimensionless quantity akin to a Rayleigh number has to overcome some critical value R_c. As the initial temperature increase ΔT is proportional to the square of the planetary radius R (see Eq. (1)) and the gravity g, to R, the condition (11) implies that the melting proceeds when

$$R > A\left(\frac{R_D}{R}\right)^{-3/8}, \tag{12}$$

where A is an appropriate dimensional constant, $A^8 = (27 R_c f_2^2 C^2\, \mu_m\kappa (T_M - T_0)^2) / (16\Delta\rho\pi^3 G^3 \bar{\rho}^3 f_1^2)$. Of course R has also to be large enough (here 1762 km) that the temperature in the impact zone is larger than T_{melt}. This relation is in satisfactory agreement with the Fig. 4 (an exponent of -0.3 is observed rather than $-3/8 = -0.37$).

The radius at which this instability occurs is related to the initial temperature of the impacted body. However, as the temperature in the impacted zone varies with R^2, the dependence on the initial temperature is weak and it is difficult to avoid melting before a Mars-size embryo. In all cases, we predict a proto-core formation in an early stage of planetary evolution and at rather low pressure (10–20 GPa) when the proto-core mass is less than 10% of that of the present-day Earth. Most of the core mass of large differentiated planets is added subsequent to the situation described in this paper by a still ongoing accretion of planetesimals and of differentiated embryos.

The previous simulation assumes that the growing planetary embryo is homogeneous. There are however various indications that some planetesimals can start melting and differentiating in the first million years of accretion due to the presence of short period radionuclides (e.g. Rubie et al., 2007). These small planetesimals

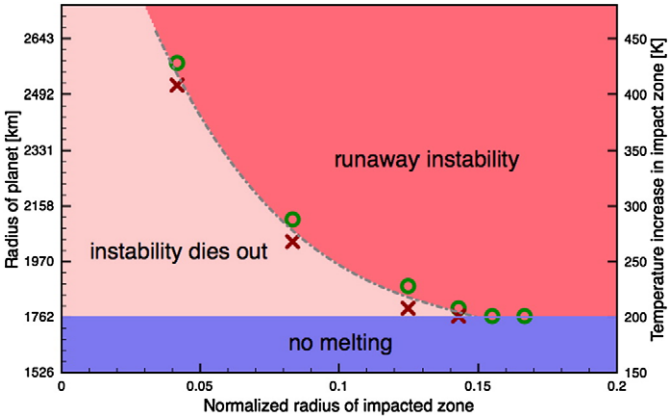

Fig. 4. Regime map of the runaway instability: various numerical experiments have been performed by varying the radius of the impacted zone (normalized by the planet radius, horizontal axis) and the planet radius (left axis, and consequently the temperature increase after the impact, right axis, see (1)). For a too small planet the iron melting temperature is never reached (blue). For a too small impacted zone (peach) the instability dies out. For large enough planets and impactors the runaway core formation occurs until the whole proto-planet is differentiated (red). The green and red symbol report numerical simulations that constrain the threshold of instability (dashed line). (For interpretation of the references to colour in this figure legend, the reader is referred to the web version of this article.)

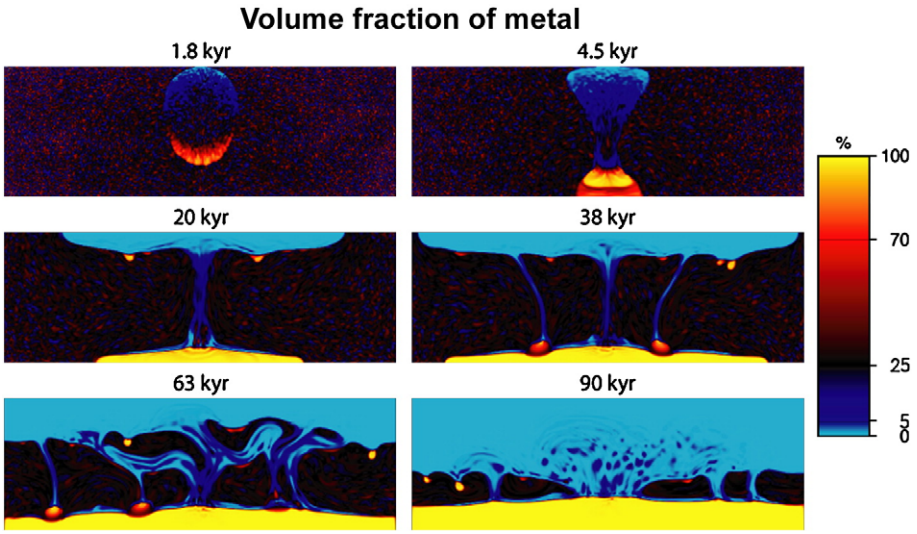

Fig. 5. A runaway differentiation very similar to Fig. 2 is also predicted in simulations of large aspect ratio and non uniform composition.

loose their heat sources and can cool rapidly if they are not too large (the half-life of ^{26}Al is only 0.75 myrs). The planetary embryos are therefore probably built from a mixture of solid planetesimals that have undergone various stages of differentiation. The evolution of a growing planet embryos made up of differentiated materials is controlled by the characteristic sizes of the compositional metal/silicate heterogeneities. If large volumes of differentiated metal were accreted (typically with radii larger than ~10 km), their Stokes velocities were large enough that they started sinking before the embryo radius reached 2000 km. In this case the choice of an initial homogeneous composition may not be realistic. On the other hand, if the building bricks of embryos were small planetesimals or small fragments of large planetesimals broken into small pieces during their impacts, then no significant differentiation could have occurred without melting within the duration of a few 10 myrs expected for core formation.

To check that the segregation scenario described in Fig. 2 would remain the same in a non-homogeneous planet embryo and with a different aspect ratio, we performed another simulation shown in Fig. 5. We choose a volume of aspect ratio 3 and an initial composition where the metal content varies locally between 1% and 90%, with a random distribution with exponential deviate and an average value of 25% metal like in Fig. 2. Because the initial density is not uniform, the initial velocity is non zero, but very small, before an impact. As soon as the impact occurs, the destabilization of the planet follows in a way very similar to what is obtained with a uniform planet embryo (compare Figs. 2 and 5). The only difference is that the initial random distribution of metal leads to a somewhat more complex and less symmetric pattern of differentiation controlled by the initial granularity of metal distribution.

The core formation predicted by our formalism and numerical model is significantly different from previous scenarios (Rubie et al., 2003): it is a catastrophic and early event that occurs without the mid-mantle temporary storage of metal ponds. The segregation occurs during the phase of oligarchic growth in Moon to Mars-sized planetary embryos as soon as the iron melting temperature is reached and while the silicates are still solid. The first diapir that crosses the mantle leaves a trailing conduit that connects the proto-core to the near surface silicates across the undifferentiated material. The highest temperatures are reached in the conduit itself that might have provided during the rest of the accretion, an easy path for metal transport from the near-surface regions to the core. The sinking of metal is very fast (~10 kyr) as the flow is intermediate between a diapir and a porosity wave with silicates and metal travelling in opposite directions (see Fig. 1). The release of gravitational energy increases the temperature both in the proto-core and in the shallow silicate mantle, and leaves a rather cold deep undifferentiated mantle. The overheated core carries about a half of the accretionary heat and cannot dispose of it by thermal convection in the short time scale of core formation; partial melting of silicates might have thus occurred in the deep mantle (Labrosse et al., 2007). The cores of large planets are not the result of segregation in the large planets themselves, but have been formed by merging the cores of already differentiated embryos.

Acknowledgments

We thank T. Gerya and two anonymous reviewers for their constructive comments. This work has been supported by the French ANR program ETHER.

Appendix A. Supplementary data

Supplementary data associated with this article can be found, in the online version, at doi:10.1016/j.epsl.2009.04.021.

References

Benz, W., Cameron, A.G.W., 1990. Terrestrial effects of the giant impact. In: Newsom, H.E., Jones, J.H. (Eds.), Origin of the Earth. InOxford University Press, New York, pp. 61–67.
Bercovici, D., Ricard, Y., March, 2003. Energetics of a two-phase model of lithospheric damage, shear localization and plate boundary formation. Geophys. J. Int. 152 (3), 581–596.
Bercovici, D., Ricard, Y., Schubert, G., May, 2001. A two-phase model for compaction and damage, Part 1: General theory. J. Geophys. Res. 106 (B5), 8887–8906.
Canup, R.M., Asphaug, E., 2001. Origin of the moon in a giant impact near the end of the earth's formation. Nature 412, 708–712.
Carlson, R.W., Langmuir, G.W., 2000. Timescales of planetesimal formation and differentiation based on extinct and extant radioisotopes. In: Canup, R.M., Righter, K. (Eds.), Origin of the Earth and Moon. InUniversity of Arizona Press, Tucson, pp. 25–44.
Flasar, F.M., Birch, F., 1973. Energetics of core formation: a correction. J. Geophys. Res. 78, 6101–6103.
Gerya, T.V., Yuen, D.A., 2007. Robust characteristics method for modelling multiphase visco-elastic thermo-mechanical problems. Phys. Earth Planet. Inter. 163, 83–105.
Golabek, G.J., Schmeling, H., Tackley, P.J., 2008. Earth's core formation aided by flow channelling instabilities induced by iron diapirs. Earth Planet. Sci. Lett. 271, 24–33.
Harten, A., March, 1983. High resolution schemes for hyperbolic conservation laws. J. Comp. Phys. 49 (3), 357–393.
Hier-Majumder, S., Ricard, Y., Bercovici, D., August, 2006. Role of grain boundaries in magma migration and storage. Earth Planet. Sci. Lett. 248 (3–4), 735–749.
Höink, T., Schmalzl, J., Hansen, U., September, 2006. Dynamics of metal-silicate separation in a terrestrial magma ocean. Geochem. Geophys. Geosyst. 7 (9), Q09008.

Honda, R., Mizutani, H., Yamamoto, T., February, 1993. Numerical simulation of Earth's core formation. J. Geophys. Res. 98 (B2), 2075–2089.
Kaula, W.M., 1979. Thermal evolution of Earth and Moon growing by planetesimal impacts. J. Geophys. Res. 84 (NB3), 999–1008.
Kokubo, E., Ida, S., 1996. On runaway growth of planetesimals. Icarus 123, 247–257.
Kokubo, E., Ida, S., 1998. Oligarchic growth of protoplanets. Icarus 131, 171–178.
Labrosse, S., Hernlund, J.W., Coltice, N., 2007. A crystallizing dense magma ocean at the base of the earth's mantle. Nature 450, 866–869.
Li, J., Agee, C.B., June, 1996. Geochemistry of mantle–core differentiation at high pressure. Nature 381 (6584), 686–689.
Matsui, T., Abe, Y., November, 1986a. Formation of a 'magma ocean' on the terrestrial planets due to the blanketing effect of an impact-induced atmosphere. Earth Moon, Planets 34 (3), 223–230.
Matsui, T., Abe, Y., August, 1986b. Impact-induced atmospheres and oceans on Earth and Venus. Nature 311 (6079), 526–528.
McKenzie, D., 1984. The generation and compaction of partially molten rock. J. Petrol. 25, 713–765.
Melosh, H.J., 1996. Impact cratering: a geologic process. Oxford University Press, New York.
Monteux, J., Coltice, N., Dubuffet, F., Ricard, Y., December, 2007. Thermo-mechanical adjustment after impacts during planetary growth. Geophys. Res. Lett. 34 (L24201).
Olson, P., Weeraratne, D., 2008. Experiments on metal-silicate plumes and core formation. Philos. Trans. R. Soc. Lond., A 366, 4253–4271.
Pierazzo, E., Vickery, A.M., Melosh, H.J., June, 1997. A reevaluation of impact melt production. Icarus 127 (2), 408–423.
Ricard, Y., Bercovici, D., Schubert, G., 2001. A two-phase model for compaction and damage 2. Applications to compaction, deformation, and the role of interfacial surface tension. J. Geophys. Res. 106, 8907–8924.
Rubie, D.C., Melosh, H.J., Reid, J.E., Liebske, C., Righter, K., January, 2003. Mechanisms of metal-silicate equilibration in the terrestrial magma ocean. Earth Planet. Sci. Lett. 205 (3–4), 239–255.
Rubie, D., Nimmo, F., Melosh, H., 2007. Treatise on Geophysics. Vol. vol 9. G. Schubert, Ch. Formation of the Earth's core, pp. 51–90.
Samuel, H., Tackley, P.J., 2008. Dynamics of core formation and equilibrium by negative diapirism. Geochim. Geophys. Geosys. 9, Q06011.
Scott, D.R., Stevenson, D.J., November, 1984. Magma solitons. Geophys. Res. Lett. 11 (11), 1161–1164.
Senshu, H., Kuramoto, K., Matsui, T., December, 2002. Thermal evolution of a growing Mars. J. Geophys. Res. 107 (E12), 5118.
Solomatov, V.S., 2000. Fluid dynamics of a terrestrial magma ocean. In: Canup, R.M., Righter, K. (Eds.), Origin of the Earth and Moon. InUniversity of Arizona Press, Tucson, pp. 323–338.
Solomon, S.C., June, 1979. Formation, history and energetics of cores in the terrestrial planets. Phys. Earth Planet. Inter. 19 (2), 168–182.
Spiegelman, M., January, 1993. Physics of melt extraction: theory, implications and applications. Trans. R. Soc. Lond. A 342 (1663), 23–41.
Sramek, O., 2007. Modèle d'écoulement biphasé en sciences de la terre: fusion partielle, compaction et différenciation,. Ph.D. thesis, Ecole Normale Supérieure de Lyon.
Šrámek, O., Ricard, Y., Bercovici, D., March, 2007. Simultaneous melting and compaction in deformable two-phase media. Geophys. J. Int. 168 (3), 964–982.
Stevenson, D.J., 1981. Models of the earth's core. Science 214, 611–619.
Stevenson, D.J., 1990. Fluid dynamics of core formation. In: Newsom, H.E., Jones, J.H. (Eds.), Origin of the Earth. InOxford University Press, pp. 231–249.
Tonks, W.B., Melosh, H.J., March, 1993. Magma ocean formation due to giant impacts. J. Geophys. Res. 98 (E3), 5319–5333.
Touboul, M., Kleine, T., Bourdon, B., Palme, H., Wieler, R., 2007. Late formation and prolonged differentiation of the Moon inferred from W isotopes in lunar metals. Nature 450, 1206–1209.
von Bargen, N., Waff, H.S., 1986. Permeabilities, interfacial areas and curvatures of partially molten systems: Results of numerical computation of equilibrium microstructures. J. Geophys. Res. 91 (B9), 9261–9276.
Yin, Q.Z., Jacobsen, S.B., Yamashita, K., Blichert-Toft, J., Télouk, P., Albarède, F., August, 2002. A short timescale for terrestrial planet formation from Hf–W chronometry of meteorites. Nature 418 (6901), 949–952.
Yoshino, T., Walter, M.J., Katsura, T., 2003. Core formation in planetesimals triggered by permeable flow. Nature 422, 154–157.